Interferometric Measurements of Refractive Index Dispersion in Polymers over the Visible and Near-Infrared Spectral Range

Sarah E. Caudill, W. Tandy Grubbs

Department of Chemistry, Stetson University, DeLand, Florida 32720

Received 29 March 2005; accepted 16 July 2005
DOI 10.1002/app.22724
Published online 6 January 2006 in Wiley InterScience (www.interscience.wiley.com).

ABSTRACT: A low-coherence Michelson interferometric method for characterizing the refractive index and refractive index dispersion over the visible and near-infrared spectral ranges (350–1700 nm) is described. The method is particularly suited to measurements in optical materials that have flat, parallel surfaces. The accuracy and precision associated with the method are address from a theoretical standpoint and the technique is demonstrated through the collection of dispersion curves for a number of standard optical glasses and three common polymers (polystyrene, poly(methyl methacrylate), and polycarbonate). The advantages and disadvantages of this method in comparison to conventional "refractometry" (i.e., the Abbé refractometer) are also addressed. © 2006 Wiley Periodicals, Inc. J Appl Polym Sci 100: 65–72, 2006

Key words: refractive index; optics; polystyrene; polycarbonates; calculations

INTRODUCTION

The expanding use of the internet and the accompanying demand for high-bandwidth transmission media has fueled interests in "all-optical" networking. Polymers are emerging as key materials in the development of optical networks, owing to their flexibility, light weight, low cost of fabrication, and the potential to create materials with a variety of physical and optical properties.[1–3] Silica glass provides a suitable material for optical elements and is a suitable fiber optic material for transmitting data over backbone wide area networks; single-mode silica fibers possess high transmission windows centered at the near-infrared (NIR) communication wavelengths of 850, 1300, and 1550 nm. However, the use of silica fibers in local area networks (LANs) is unrealistic because of the numerous couplings that exist between the backbone wide area network and the desktop user. Less brittle, larger-diameter, polymer-based multimode fibers present an alternative to silica fibers that would be easier to couple by a field technician in a LAN environment. In general, "all-optical" networking will be promoted by the development of polymer-based waveguides, graded-index fibers, lenses, and various other linear and nonlinear optical components.

Research and development of optical polymers is currently hindered due to a lack of instrumentation for fully characterizing the bandwidth capacity of candidate materials in the visible and particularly the NIR spectral regions. There is wide interest in developing new instruments that allow one to better characterize the absolute refractive index (n), refractive index dispersion ($dn/d\lambda$), and refractive index stability of new polymeric materials in the NIR spectral region. Refractometric instruments such as the Abbé refractometer have traditionally been used for measuring n and $dn/d\lambda$, where n is determined from the angle of refraction of light according to Snell's law. Maintaining high accuracy and precision over a wide spectral range in such instruments can only be accomplished through careful calibration. Furthermore, refractometric measurements are normally restricted to liquid, gel, and thin solid samples (bulk polymer samples can be difficult to analyze with suitable accuracy and precision).

Described here is a recently constructed low-coherence Michelson interferometric apparatus that is capable of measuring refractive index over a broad spectral range (350–1700 nm). This technique is particularly suited to the study of bulk optical elements that contain flat, parallel surfaces. The interferometric apparatus utilizes a tunable arc-lamp source that is directed into a Michelson interferometer that contains two mirrors; one mirror has a fixed position and the other can be translated with a precision motorized translation

*Some literature values for refractive index, n_d, were obtained from the JDS Uniphase OCLI Products website (www.ocli.com) and from the 2004 Edmund Industrial Optics catalog.

Correspondence to: W. Tandy Grubbs (wgrubbs@stetson.edu).

Contract grant sponsor: National Science Foundation; contract grant number: DMR-0215407.

stage. Two measurements must be performed to obtain refractive index: (1) One first translates the moveable mirror until a maximum interference fringe intensity is established; fringes will only be observed if the optical pathlengths of the two arms of the interferometer do not differ by more than the coherence length of the light source (the Xenon arc-lamp/monochromator source employed here has a coherence length of ~150 μm); (2) The sample is then introduced into the fixed pathlength arm of the interferometer and the pathlength of the other arm is increased with the motorized translation stage to reestablish the maximum interference. The distance that the mirror moves to reestablish the maximum interference is defined as p (the "optical delay distance"). The refractive index (relative to air) can then be calculated from the expression

$$n_{\text{sample}} = n_{\text{air}} + p/l \quad (1)$$

where l is the thickness of the optical sample and n_{air} is the refractive index of the air displaced by the sample in the interferometer. Since n_{air} is nearly equal to 1, $(1 + p/l)$ represents a practical measure of index that is suitable for many optical design applications. Alternatively, more precise absolute indexes can be obtained if the exact value of n_{air} is known for the wavelength of light under consideration.

Instead of using the "two measurement" technique described earlier, we are able to obtain p in a single scan by positioning the sample in the interferometer in such a way that it eclipses approximately half the low-coherence light beam image. Consequently, two interference wave packets are observed as the mirror is translated; one corresponds to light traveling through the sample and one corresponds to light traveling next to the sample (through air). The optical distance between the two interference wave packets yields an experimental measure of p.

Interferometric methods of determining both absolute and differential refractive index have been attempted previously in our lab[4,5] and by others.[6–11] Many of these approaches are based upon some form of low-coherence interferometry (or white-light interferometry), where a low-coherence arc-lamp source is used to illuminate the sample. The primary challenge associated with low-coherence methods is the accurate identification of the central oscillation in the experimentally collected interference wave packet[7,8,10,12–14]; uncertainty in locating the center of the wave packets yields corresponding uncertainties in the refractive index. One approach to minimizing the error in locating the central oscillation is to use a dual wavelength illumination source[8,14]; the two wavelengths interfere within the region of the interference wave packet (at their "beat frequency"), which makes the central oscillation more pronounced. Our approach in the current study is to take advantage of several recent technological advances that in turn improve the signal-to-noise and resolution of the collected low-coherence interferometry data. These advances include (1) the use of an ultra precise motorized translation stage that uses active feedback to smoothly control the acceleration and velocity of the ramping mirror in the interferometer, (2) the incorporation of an interfering frequency-stabilized helium–neon (HeNe) laser beam that is used to track the motion of the ramping mirror with better than 50-nm resolution, and (3) the use of current data acquisition hardware and software that permits the collection and analysis of interference data with high temporal resolution over an extended period of time (2–5 min).

The detailed design of the new Michelson interferometric apparatus and the data analysis protocol are described herein. The performance of the new instrument is evaluated by measuring the refractive index dispersion ($dn/d\lambda$) for a number of common inorganic and polymer window materials. The advantages and disadvantages associated with this interferometric approach in comparison to conventional refractometer are discussed.

EXPERIMENTAL

Tunable light source

Referring to Figure 1, radiation from a Xenon arc-lamp (Oriel Photomax™ with 75 W, ozone-free lamp) is disbursed with a 1/8-m monochromator (Oriel Cornerstone™ 130) yielding tunable light from the ultraviolet into the mid-infrared spectral range. The monochromator is equipped with two gratings that can be interchanged and tuned remotely through a computer controller; a 1200 lines/mm grating that is blazed for 350 nm is used to obtain light within the range 300–1000 nm and a 600 lines/mm grating that is blazed for 1000 nm is used to obtain light within the range 1000–1900 nm.

Interferometer

The light from the monochromator is directed through a custom-made Michelson interferometer, where one mirror is fixed and the other mirror can be translated with a precision motorized translation stage (Physik Instrumente M-126.DG linear positioning stage, with Mercury II C-862 single axis DC-motor controller). Aluminum coated, $\lambda/10$ flatness first-surface mirrors are used throughout the apparatus and a nonpolarizing BK7 cube beamsplitter is employed (Edmund Industrial Optics, R47–009; $\lambda/8$ flatness). Light from a frequency stabilized HeNe laser (Spectra-Physics, Model 117A) is also directed through the interferometer along a parallel optical path. During a trial, the

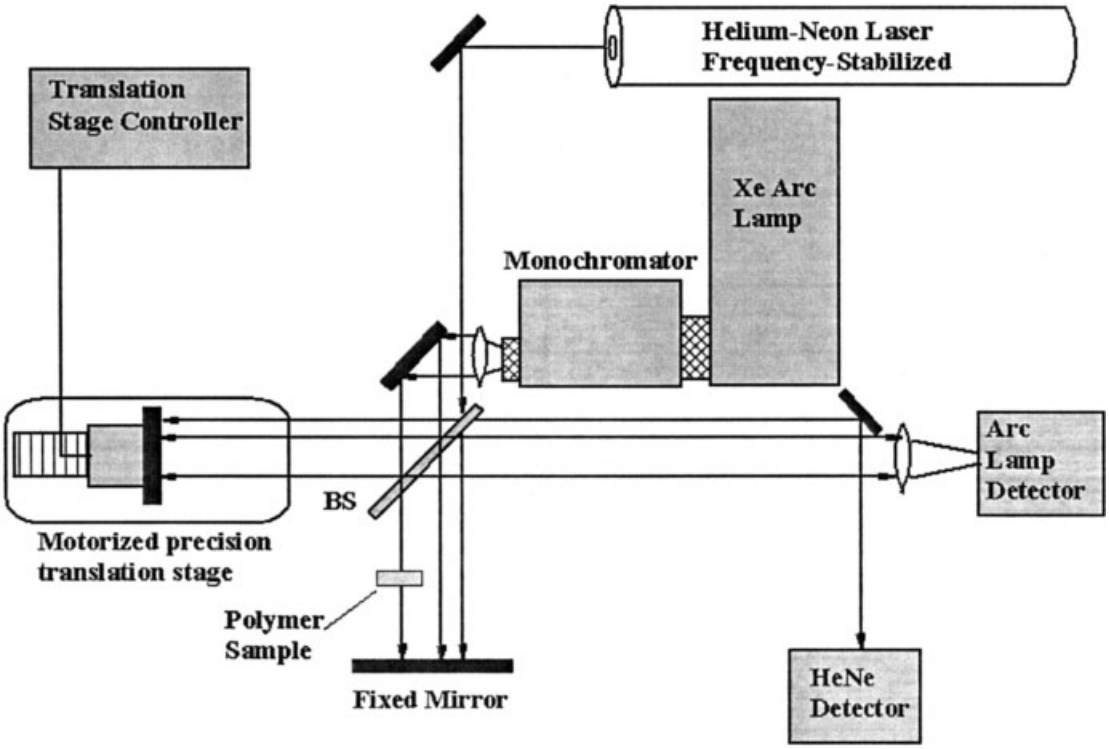

Figure 1 Schematic diagram of the low-coherence Michelson interferometer for measuring refractive index.

interference of the HeNe laser is recorded as a function of mirror displacement, simultaneous with the interference of the arc-lamp source; the alternating light and dark fringes from the HeNe source are used to make a more precise measurement of mirror displacement than what would otherwise be obtained from the stepper-motor controller of the translation stage. This means of determining mirror displacement is also advantageous because it actively accounts for any variations in optical distance in the interferometer that might arise due to thermal expansion of optical mounts. The interference intensity of the HeNe laser is monitored with a battery powered photodiode/amplifier (OPT101, Burr-Brown Corp) and the interference intensity of the arc-lamp source is detected with a photodiode (either silicon Model PDA55 for 300–900 nm light or an InGaAs Model PDA255 for 900–1700 nm; Thorlabs, Inc.) which is amplified with a preamplifier (SR560, Stanford Research Systems). The HeNe and arc-lamp interference voltages are recorded at a 250-Hz collection rate, using an analog-to-digital computer interface (LabPro, Vernier Software and Technology).

The entire interferometric apparatus is housed inside of a thermostated acrylic box (25°C) and is mounted on a vibration free optical table (VERE, Inc.). To measure refractive index, the sample of interest is mounted in one arm of the interferometer, the arc-lamp monochromator is tuned to the wavelength of interest and the interference intensities of the arc-lamp and HeNe are recorded while one mirror is translated once over the appropriate range. The Physik Instrumente M-126.DG linear positioning stage that is used to control the mirror movement utilizes an active computer-interfaced drive feature that allows the user to control the acceleration and velocity of the stage with 8.5-nm design resolution (the stage controller actively corrects for errors in displacement as it is ramped). A mirror velocity of 17 μm/s is typically used during data collection. The total distance that the mirror is displaced during a trial depends on the thickness of the optical sample and its refractive index.

Materials

Low-coherence interferometric measurements of refractive index were carried out on the following common inorganic and polymer window materials: fused silica glass, BK7 glass, Borofloat™ glass, MgF_2, polycarbonate, poly(methyl methacrylate), and polystyrene. Table I summarizes the different materials characterized in this study and also lists the source, thickness, and the literature value for the refractive index (n_d) at 589.3 nm.

Data analysis protocol

Figure 2 shows a typical computer acquisition of the arc-lamp interference over time as the mirror is trans-

TABLE I
Summary of Materials Studied in This Investigation, Indicating the Source, Thickness, and the Literature Value of the Index of Refraction at 589.3 nm

Material	Thickness (l)[a] (μm)	n_d (literature)[b]	Source
Fused silica	5997	1.458	c
BK7 glass	7410	1.517	c
Borofloat™ glass	6458	1.472	c
MgF_2	5086	1.378 (n_0)	c, d
Polycarbonate	8568	1.585	e
Poly(methyl methacrylate)	5378	1.490	f
Polystyrene	2306	1.591	g

[a] The thickness of each sample was measured with a precision caliper.
[b] n_d literature values for the inorganic glasses were obtained from the 2004 Edmund Industrial Optics® catalog (NO4RB) and literature values for the three polymer samples.
[c] Purchased from Edmund Industrial Optics®.
[d] The sample of MgF_2 used here is cut so that the optical axis is along the *c*-axis of the crystal, thereby minimizing birefringence.
[e] Lexan® Polycarbonate sheet, manufactured by GE Structured Products, Inc.
[f] Cell-cast acrylic sheet, manufactured by Spartech Polycast, Inc.
[g] Cell-cast polystyrene sheet, manufactured by Plaskolite, Inc.

lated for a magnesium fluoride sample. Two, and sometimes three, interference wave packets are observed per trace as a result of having the sample mounted in an eclipsed fashion: (1) a packet that corresponds to light passing through the sample twice (i.e., light that passes through the sample, bounces off the fixed mirror, and then passes through the sample again), (2) a middle packet can be visible that corresponds to light passing through the sample only once during its round trip, and (3) a packet that corresponds to light that never passes through the sample during its round trip. All three wave packets are clear in Figure 2. Only two packets are required to calculate refractive index; the middle packet is often small in comparison to the baseline noise and, as such, we normally use the outside packets to determine n_{sample}.

Figure 3 shows the first wave packet from Figure 2 on an expanded scale, revealing a rapid alternating intensity indicative of an optical interferogram. Fourier transformation of such packets have been carried out to verify the wavelength of our source, yielding sharply spiked frequency spectra centered at the intended wavelength of the monochromator.

Also shown in Figure 3 is the rapidly alternating light-and-dark interference signal of the HeNe laser source plotted above the arc-lamp interference. Since the wavelength of the HeNe is 632.8 nm, each full oscillation of the HeNe signal indicates a mirror translation of (½)·632.8 nm; the factor of ½ enters here because the light beam travels twice between the beam-splitter and the mirror in a Michelson interferometer design. Since the HeNe laser has an extraordinarily long coherence length (~20 cm), the alternating interference intensity of this source is not diminished over the mirror displacements used here. This is in contrast to the arc-lamp source, which has a small coherence length, meaning that interference is only observed over a short range.

For each data set, p is measured as ½ the mirror displacement between the central fringes of the outermost wave packets. The ultimate precision in determining p is limited by two factors: (1) the error in locating the central interference fringe in each packet and (2) the error in measuring the mirror displacement between these two limits. The error associated with factor (1) is dependent on the widths of the wave packets, which can be substantial even when the coherence length of the light source is on the order of a 100 μm. Coherence length is strongly dependent upon the wavelength and spectral resolution of the arc-lamp/monochromator tunable light source; the exact dependence is addressed in detail in the Theoretical Considerations section. The error associated with factor (2), measuring the mirror displacement, is minimized by defining displacement relative to the number of fringes that pass in the HeNe laser interference signal; this total length is therefore defined as a multiple of the HeNe wavelength, meaning the method possesses an inherent length standard.

The following data analysis protocol was used to determine a refractive index value from each data set:

1. The raw data is exported for manipulation into a quantitative analysis software environment (Mathcad 2001, Mathsoft Corp., is used here).
2. The data encompassing the arc-lamp interference around each interference wave packet is sepa-

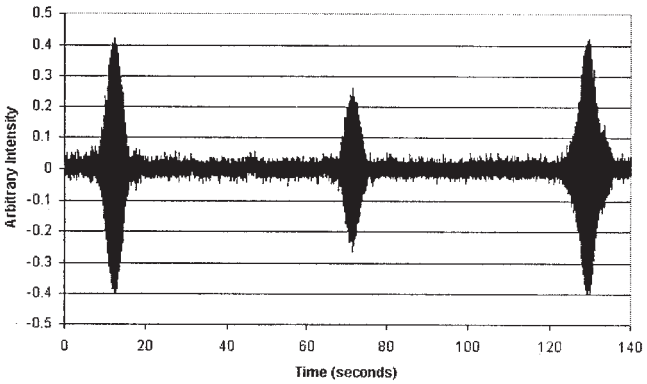

Figure 2 Typical interference trace for a MgF_2 plate (light source tuned to λ = 790.0 nm and sample thickness = 5086 μm). The individual oscillations within each wave packet occur at such a large frequency that they cannot be observed on the temporal scale used here.

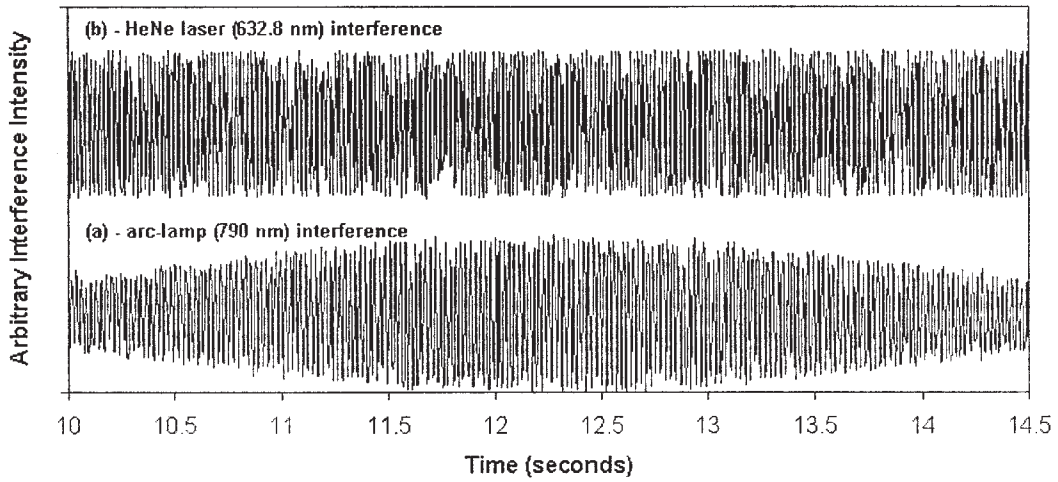

Figure 3 Plot (a) shows a blow-up of the first arc-lamp interference wave packet in Figure 2. Plot (b) shows the corresponding oscillations in the HeNe laser interference that are used to determine the distance that the mirror translates during a scan.

rated from the original data set and each is processed with an algorithm that extracts the data points corresponding to the maximum voltage of each oscillation These maxima, when plotted against time, have a Gaussian distribution.

3. The wave packet envelopes from (2) are each fitted to a Gaussian function to determine the temporal location of the maximum (hereafter, the maximum time associated with the first wave packet is called t_1 and with the second wave packet is called t_2).
4. The HeNe interference signal data set that was collected simultaneous with the above data is then analyzed with a separate algorithm that counts the number of maxima that appear between times t_1 and t_2. This method yields the number of HeNe fringes that pass between these two times and will hereafter be called N.
5. Refractive index is finally calculated as $n = 1 + N \times 0.6328165/(2l)$, where l is the thickness of the sample (measured independently with a precision caliper) and the factor of 0.6328165 is the manufacturer's value for the wavelength in air of the HeNe laser in units of micrometers.

Theoretical considerations

A number of experimental parameters affect the width of the experimentally recorded interference wave packets. Under certain circumstances, these widths can be substantial which in turn limits the precision associated with the measurement of refractive index by this method. A theoretical expression for the interference wave packet is derived later, which shows explicitly how the wave packet width depends on the wavelength and spectral width of the illumination light source.

As stated above, the Xe arc-lamp/monochromater light source delivers tunable light from 300 to 1900 nm. The monochromator is also equipped with adjustable, micrometer-driven entrance and exit slits. The ultimate output of this arc-lamp/monochromator combination is well described by a Gaussian spectral envelop centered at λ_{max} with a $1/e$ half-width equal to $\Delta\lambda$. $\Delta\lambda$ can be increased or decreased by opening or closing the entrance and exit slits of the monochromator (the minimum slit width setting corresponds to a $\Delta\lambda$ of 0.2 nm, although the amount of light escaping the monochromator at this slit setting is too small for visual alignment of the optical elements in the interferometer. The typical slit settings used during our measurements correspond to a $\Delta\lambda$ value of 5 nm.

An analytical expression for the interference wave packet is more easily obtained by expressing the Gaussian spectral envelop in units of wave numbers ($\bar{v}$) according to

$$I(\bar{v}) = A \exp\left[-\left(\frac{\bar{v} - \bar{v}_{max}}{\Delta\bar{v}}\right)^2\right], \qquad (2)$$

where A is the amplitude at the spectral maximum, $\bar{v}_{max} = 1/\lambda_{max}$,, and $\Delta\bar{v} = \Delta\lambda/(\lambda_{max})^2$. Each wave number component of the incident light source ($(\bar{v})$) will give rise to interference intensity oscillations as a function of mirror displacement (p) according to the expression $[1 + \cos(2\pi\bar{v}p)]$. The overall interference wave packet is obtained by integrating this cosine function over the incident spectral envelop; specifically, the interference intensity as a function of mirror displacement (p) is given by

$$I(p) = \int_0^\infty I(\bar{v})[1 + \cos(2\pi\bar{v}p)]d\bar{v}. \qquad (3)$$

An analytical solution to this integral can be obtained by centering the integration around the maximum of the Gaussian spectral envelop by defining $x = \bar{v} - \bar{v}_{max}$ and extending the integration from $-\infty$ to $+\infty$. Equation (3) then becomes

$$I(p) = A\int_{-\infty}^{\infty} \exp\left[-\left(\frac{x}{\Delta\bar{v}}\right)^2\right]\{1 + \cos[2\pi(x + \bar{v}_{max})p]\}dx. \quad (4)$$

Using the trigonometric relationship

$$\cos[2\pi(x + \bar{v}_{max})p] = \cos(2\pi xp)\cos(2\pi\bar{v}_{max}p) - \sin(2\pi xp)\sin(2\pi\bar{v}_{max}p), \quad (5)$$

the integral can then be solved piecemeal, yielding

$$I(p) = A\sqrt{\pi}\Delta\bar{v}\{1 + \cos(2\pi\bar{v}_{max}p)\exp[-(\pi\Delta\bar{v}p)^2]\}. \quad (6)$$

Inspection of eq. (6) reveals that the overall envelop of the interference wave packet is described by the Gaussian term $\exp[-(\pi\Delta\bar{v}p)^2]$,, which possesses a $1/e$ width of $1/(\pi\Delta\bar{v})$.. Converting back to wavelength units, the $1/e$ width of a wave packet is given by

$$\Delta p = \frac{\lambda_{max}^2}{\pi\Delta\lambda}. \quad (7)$$

Therefore, the width of an experimentally measured interference wave packet is dependent on the square of the incident wavelength maximum and is inversely proportional to the width of the spectral envelop. As such, the inherent precision in locating an interference wave packet maximum will degrade as the wavelength of the light source is tuned to longer wavelengths and as the entrance and exit slits of the monochromator are closed down (spectral resolution will have to be sacrificed to improve the precision of an interferometric determination of refractive index). This fact is illustrated in Figure 4, which shows several plots of eq. (6), illustrating how the width of the Gaussian wave packet increases with increasing λ_{max} and decreasing $\Delta\lambda$.

Equation (7) can also be used to estimate the precision in our measurement of refractive index (and how this precision varies with λ_{max} and $\Delta\lambda$). Assuming that the center of the two Gaussian wave packets in a scan can be identified to within $\pm 10\%$ of the $1/e$ widths described by eq. (7), the propagated error in our measurement of p is given by

$$\delta p = \frac{\sqrt{2}}{10}\frac{\lambda_{max}^2}{\pi\,\Delta\lambda}. \quad (8)$$

The corresponding precision in the measured refractive index is given by $\delta n = \delta p/l$. If, for example, one is investigating a 4-mm thickness optical element at the wavelengths λ_{max} = 400, 1000, and 1600 nm, the entrance and exit slits of the monochromator would have to be adjusted to yield $\Delta\lambda$ values of 9, 56, and 144 nm, respectively, to obtain a refractive index precision of ± 0.0002 units.

The accuracy associated with measurements of refractive index by interferometry is primarily limited by the uncertainty in the sample thickness, l, which can usually only be measured to within 5 μm with a precision micrometer. The actual magnitude of this systematic error is given by

$$\delta n = \left(\frac{p}{l^2}\right)\delta l, \quad (9)$$

indicating that the accuracy is improved as the thickness of the optic is increased. For an optical element with hypothetical index equal to 1.4, the systematic error in measured index due to a ± 5 μm uncertainty in thickness is ± 0.07, ± 0.007, and ± 0.0014 for thicknesses of 100, 1000, and 5000 μm, respectively.

RESULTS

Figure 5 shows the variation in experimental refractive index for the polycarbonate sample over the wavelength range 400–1600 nm. Beyond 1600 nm, the precision in locating the interference wave packet maxima is degraded to a sufficient extent that further measurements become impossible. This limit in our spectral tuning range was realized for all the materials studied here.

The discrepancy between the literature values of refractive index (n_d, measured at 589.3 nm) for these materials and the interferometrically measured values carried out here are well described in terms of the uncertainty in the sample thickness according to eq. (9). "Normal" dispersion is often described for a material in terms of the empirical Cauchy formula[15]

$$n = c_0 + c_1\frac{1}{\lambda^2} + c_2\frac{1}{\lambda^4}. \quad (10)$$

We have offset our measured refractive index values so that the value at 589.3 nm agrees with the literature n_d* values,[16] and have subsequently fit the dispersion curves to eq. (10); Table II list the coefficients that were obtained for this fitting for each material.

CONCLUSIONS

A new method for measuring refractive index and refractive index dispersion has been demonstrated.

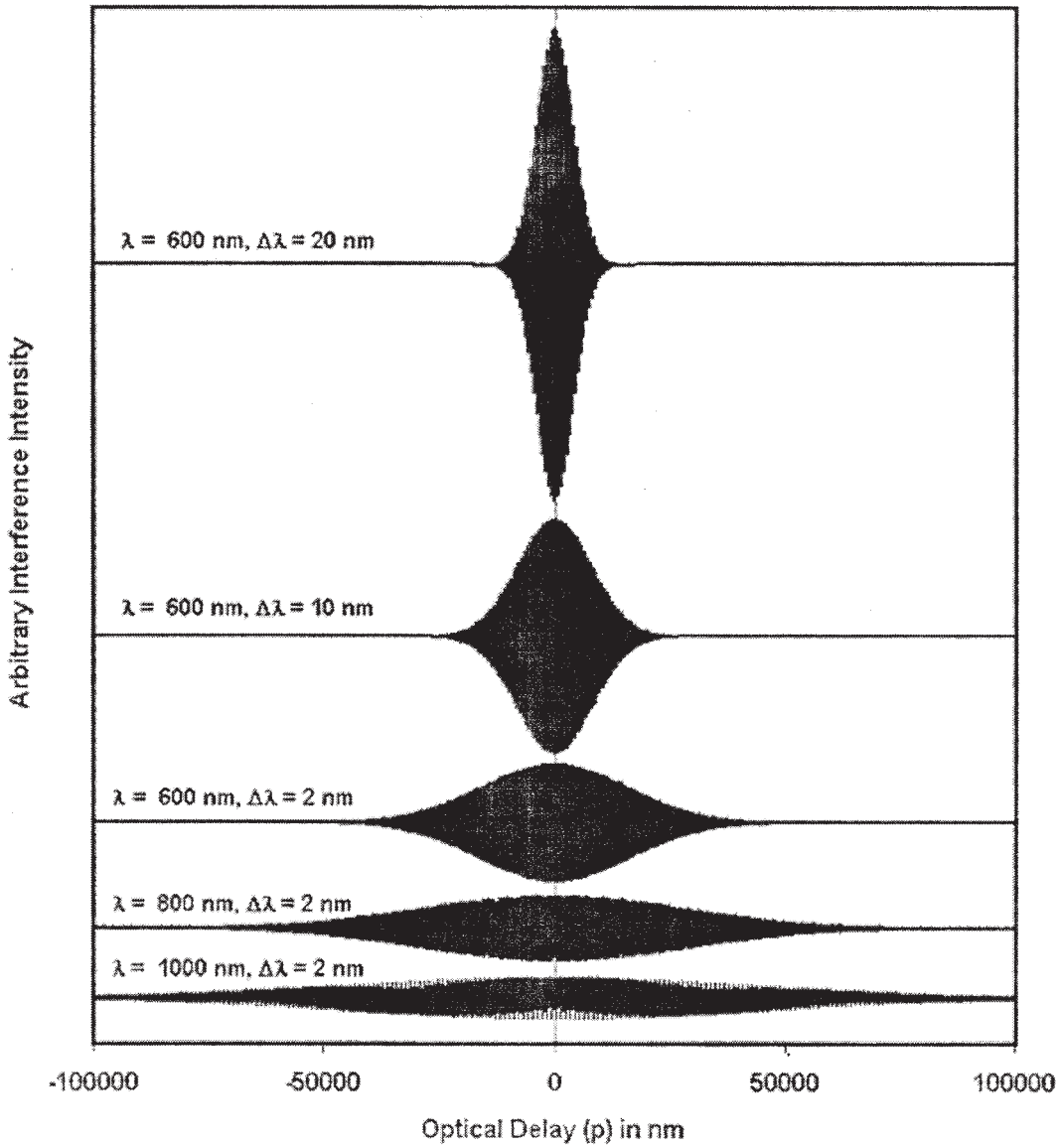

Figure 4 Theoretical plots of eq. (6), illustrating how the width of the interference wave packet increases with increasing wavelength and decreasing breadth of the spectral envelop. The actual oscillations within each wave packet, occurring at wavelength $1/\bar{v}_{max}$, cannot be observed on the scale of this plot.

The method is particularly suitable for characterizing the refractive index properties of bulk optical elements in the NIR spectral range; the spectral region that is in most optical communication devices. The accuracy and precision associated with this technique is comparable to (and can potentially exceed) standard refractometric methods when investigating samples of sufficient thickness and when illuminating the sample with a broad enough spectral envelop. The advantages associated with the method include the fact that the interferometric apparatus is tunable and does not require calibration prior to use; the optical pathlength associated with light traveling through the sample is measured relative to the wavelength of a frequency stabilized HeNe laser (the method possesses an inher-

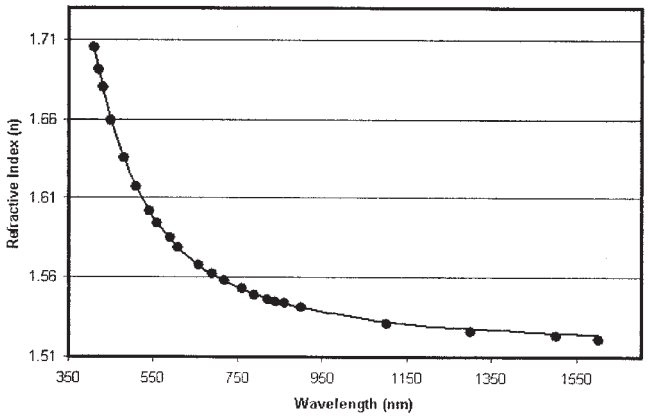

Figure 5 Variation in refractive index over the wavelength range 400–1600 nm for a bulk polycarbonate sample (thickness = 8.568 mm). The solid line is an empirical fit to the data based on eq. (10).

TABLE II
Experimental Coefficients of Dispersion according to Eq (10) (evaluated over the range 400-1600 nm)

Sample	c_0	c_1 (10^{-4})	C_2 (10^{-8})
Fused silica	1.425	1.174	−1.417
BK7 glass	1.487	0.9418	3.974
Borofloat™ glass	1.447	0.7681	3.461
MgF_2	1.368	0.3666	1.486
Polycarbonate	1.518	1.544	26.75
Poly(methyl methacrylate)	1.449	1.597	−5.529
Polystyrene	1.499	3.020	6.178

ent length standard). The incorporation of the HeNe standard also actively corrects for any errors in optical pathlength that might arise from vibrations and/or thermal expansion of optical elements in the apparatus. Disadvantages include the sensitivity of the apparatus to room vibrations (a vibration free optical table must be utilized) and the collection and analysis of the data is more laborious to accomplish with interferometry in comparison to common refractometric methods.

This project was funded by the National Science Foundation (DMR-0215407). Any opinions, findings, and conclusions or recommendations expressed in this material are those of the author(s) and do not necessarily reflect the views of the National Science Foundation.

References

1. Chowdhury, J. Chem Eng 1987, 94, 14.
2. Zubia, J.; Arrue, J. IEEE Proc Optoelectron 1997, 144, 397.
3. Garito, A. F.; Wang, J.; Gao, R. Science 1998, 281, 962.
4. Dudi, O.; Grubbs, W. T. J Appl Polym Sci 1999, 74, 2133.
5. Fogleman, E. A.; Kelly, M. T.; Grubbs, W. T. Dental Mater 2002, 18, 324.
6. Varelas, D.; Iocco, A.; Limberger, H. G.; Salathe, R. P.; Vasiliev, S. A.; Dianov, E. M.; Medvedkov, O. I.; Protopopov, V. N. Opt Lett 1999, 24, 1106.
7. Giniunas, L.; Danielius, R.; Karkockas, R. Appl Opt 1999, 38, 7076.
8. Rao, Y. J.; Jackson, D. A. Meas Sci Technol 1996, 7, 981.
9. Pliskin, W. A.; Conrad, E. E. IBM J Res Dev 1964, 8, 43.
10. Fukano, T.; Yamaguchi, I. Appl Opt 1999, 38, 4065.
11. Murphy, D. F.; Flavin, D. A. Appl Opt 2000, 39, 4607.
12. Rao, Y. J.; Jackson, D. A.; Jones, R.; Shannon, C. J Lightwave Technol 1994, 12, 1685.
13. Rao, Y. J.; Ning, Y. N.; Jackson, D. A. Opt Lett 1993, 18, 462.
14. Chen S.; Grattan K. T. V.; Meggitt, B. T.; Palmer, A. W. Electron Lett 1993, 29, 334.
15. Jenkins, F. A.; White, H. E. Fundamentals of Optics; McGraw-Hill: New York, 1976; p 479.
16. Brandrup, J.; Immergut, E. H.; Grulke, E. A., Eds.; Polymer Handbook, 4th ed.; Wiley: New York, 1999; p VI/578.